Contents lists available at Egyptian Knowledge Bank

Labyrinth: Fayoum Journal of Science and Interdisciplinary Studies

Journal homepage: https://lfjsis.journals.ekb.eg/

Review article

Review on Physics and Modelling of THz Radiation Detection Using Field-effect Transistors

Yasmeen A. Mohamed[a*], Nihal Y. Ibrahim [b], Mohamed Y. F. El Zayat [a], Salah E. A. Elnahwy [b]

[a] *Physics Department, Faculty of Science, Fayoum University, El Fayoum 63514, Egypt.*
[b] *Department of Engineering Physics and Mathematics, Faculty of Engineering, Cairo University, Giza, Egypt.*

ARTICLE INFO

Keywords:
TeraFETs
Plasma Wave Model
Hydrodynamic Model
Boltzmann Transport Model
Phenomenological Model
Equivalent circuit model

ABSTRACT

Despite the advantages of semiconductor field-effect transistors (FETs), they have yet to show competing responses in terahertz (THz) radiation detection compared to other techniques. It is therefore important to improve our understanding of the FET operation when detecting THz radiation beyond its cut-off frequency. The journey of modeling THz detection in FET started with the plasma wave model by Dyaknov and Shur and proceeded to other approaches to develop a physics-based model of the FET nonlinearity that drives the high-frequency rectification. This work presented a review of the models developed to model the operation of FEET detectors. The common factors as well as the advantages of each model are emphasized. The more we understand these models, the better we can guide the development of FET designs for higher detection responses.

1. Introduction

Terahertz (THz) detection technology has become increasingly significant over the past few decades in a variety of fields, including security and industrial imaging, space exploration, and many other applications [1]. Consequently, the need for more sensitive terahertz detectors is increasing. A terahertz detector captures electromagnetic radiation with a terahertz frequency (0.3-3 THz) and transforms it into an electric signal [2].

Multiple important devices use THz detection technologies such as microbolometers [3, 4], Golay cells, and Superconducting Tunneling Junctions (STJ) [5]. However, field-effect transistors (FETs) are one of the promising candidates for THz detection. THz detectors based on FETs (TeraFETs) offer room temperature operation, fast response time, and very high integration and functionality levels, which are required for future large sensor arrays and terahertz (THz) imaging systems [6].

The FET is a three-terminal device that regulates the current flow through its channel using a gate-controlled electric field (see **Fig. 1**). The principle behind THz radiation detection in a FET device beyond its cut-off frequency is based on the nonlinear properties of the transistor [7,8]. Different types of FETs, such as Schottky diodes [9], Metal Oxide Semiconductor Field Effect Transistors (MOSFETs) [10-13], Heterostructure Bipolar Transistors (HBTs) [14,15], and High Electron Mobility Transistors (HEMTs) (e.g. GaAs-based commercial HEMTs [16], nitride-based HEMTs [17,18], and gated double quantum well heterostructures [19]) were used to detect the THz radiation.

While the literature on THz detectors agrees that the inherent nonlinearity within a FET is the main driver for its operation as a rectifier, multiple approaches have been considered for modelling THz rectification. In this work (section 2), we present a review of different models used to describe THz rectification beyond the cut-off frequency and the physics supporting them. And in section 3 we will discuss how these models include the effect of coupling the externally applied radiation to the intrinsic device and how that can affect the overall response. It is important to better understand the physics behind the FET's responses to improve its performance.

* Corresponding author.
E-mail address: yak00@fayoum.edu.eg (Y. Mohamed); Tel.: +201001587028
DOI: 10.21608/ifjsis.2023.302842
Received 10 March 2023; Received in revised form 8 April 2023; Accepted 8 April 2023
Available online 26 April 2023

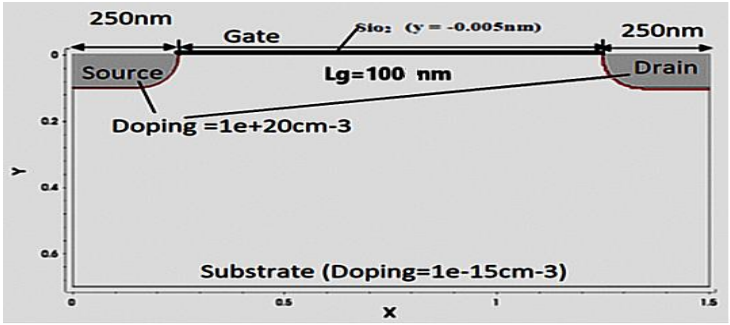

Fig. 1. The structure of the simulated Si MOSFET device[11].

2. Modelling THz radiation detection in FETs

The proposed theoretical models for THz radiation detection in a FET started with the plasma wave model by Dyaknov and Shur [20], who postulated that a FET can be a resonator of plasma spreading through the channel and that THz radiation can be detected using the nonlinear characteristics of these plasma waves. According to their work, the hydrodynamic formulas for shallow water waves can be used to explain the transistor's behaviour [20, 21]. However, recent research has opted to use the more comprehensive hydrodynamic model. Due to its complexity, the hydrodynamic model has been used mostly in simulation models, as it is harder to adapt in analytical models.

Another approach to modelling TeraFETs is the Boltzmann transport-based approach, which has been effectively used in the theoretical literature [22]. This approach includes the equivalent circuit model which represents the FET's channel as a non-quasi-static (NQS) distributed element device [23], or a nonlinear transmission line (TL) model [24]. One of the advantages of the equivalent circuit model is the possibility of integrating it into other circuits or device simulators, such as SPICE (Simulation Program with Integrated Circuit Emphasis) [25]. It can also integrate the external loading effects with the intrinsic channel response.

Another important approach that can describe the non-resonant detection of the FET detector is the phenomenological model [26]. The phenomenological model describes the FET THz rectification in terms of the device output, and it can also relate the photoresponse to the DC channel conductivity.

In the following sections, we will review and discuss these models and their differences, as well as identify their advantages and disadvantages.

2.1. Plasma Wave Theory

This is the first theory for THz detection in FET proposed by Dyaknov and Shur [20]. It relies on the THz radiation's excitation of plasma waves in the FET's channel to produce a DC output [16,27,28]. However, this perception conflicts with the conventional theoretical concept of plasma. Nevertheless, this theory has been adopted in many works [29, 30]. In this model, the Euler equation is used with the continuity equation to describe the 2D plasma in the channel, which is a known approximation for the transport charge in the channel's electron gas.

$$\partial V_g/\partial t + \partial(V_g v)/\partial x = 0 \quad \text{Euler equation} \quad (1)$$

$$\partial n/\partial t + \nabla.(nv) = 0 \quad \text{Continuity equation} \quad (2)$$

Where V_g is the effective gate-to-channel voltage ($V_g = V_{gs} - V_{Th}$), V_{Th} is the threshold voltage, V_{gs} is the applied DC gate to source voltage, $\frac{\partial V_g}{\partial t}$ is the longitudinal electric field, v is the drift velocity, and n is the charge density. Under the boundary conditions of an open drain, the solution of those equations was given in Ref. [29, 30] as,

$$\Delta V = (V_a^2/4\,V_g)F \quad (3)$$

where $\Delta V \approx V_a \cos \omega t$ is the incident drain-to-source voltage [10] such that $V_g = V_{gs0} + V_a \cos \omega t$, V_a is the AC gate-source amplitude, and F is a modulating function. In the case of high-frequency radiation (comparable to the plasma resonance frequency ω_0), F is frequency dependent, giving rise to resonant detection. In this case, F=f (ω) depends on two dimensionless parameters: ωτ and sτ/L_g (where L_g is the channel length, ω is the plasma oscillation frequency, τ is the relaxation time, and s is the plasma wave velocity). However, for lower frequencies ($\omega\tau < 1$), the dependence of F on ω decreases, and the FET operates as a broadband detector. In this case, F depends only on the bias and the boundary conditions.

The work of Meziani et al. [31] showed the dependence of F(ω) on the channel length.

$$\mathrm{F}(\omega) = 1/4L_g\sqrt{\frac{e\,V_g}{m}} \quad (4)$$

Their results showed that increasing the channel length dampens the response. To model the deep saturation behaviour, Veksler et al. [32] took into consideration the saturation FET model, the parameter controlling the modulation of the channel length, and the dependence of the threshold voltage on the source-bulk potential, such as:

$$\mathrm{V_{gs}}^2 = 2L_g j_g/\mu C_g \quad (5)$$

where j_g is the current density, C_g is the gate to channel capacitance, and μ is the electron mobility. It's worth noting that despite the revolutionary theoretical concepts introduced by Dyaknov and Shur, the plasma theory still lacks strong evidence. And although the Euler equation is an acceptable approximation for change transport in the FET, it's not sufficient for describing the FET operation in different structures and under different operation conditions. However, this model was the only one that addressed the intriguing resonant detection. For the broadband detection case, other alternatives have gradually attracted attention, such as the hydrodynamic model, which includes within it the Euler equation.

2.2. Hydrodynamic Model

While the above plasma wave model was based on the hydrodynamic particle behaviour, the models mentioned here depart from the plasma wave image and use the complete set of hydrodynamic equations to extract the FET response. Many studies have used the hydrodynamic model to derive an analytical equation to describe the electrical properties of teraFET detectors [33–39], while others used hydrodynamic equations within TCAD (Technology Computer-Aided Design) simulators [40-42]. The continuity equation can be described by equation (2Error! Reference source not found., while the standard hydrodynamic equation of motion [23] can be given by

$$\partial v/\partial t + v\,\partial v/\partial x + v/\tau = -(e/m)(\partial V_g/\partial x) \quad (6)$$

Zhang and Shur [43] demonstrated using the 1D hydrodynamic equations that the incoming pulse width and the response time under the long pulse mode significantly impact the response of TeraFETs to ultrashort pulse signals. They also demonstrated in [44], that p-diamond (diamond is a wide band gap material that has relatively high dielectric strength and thermal conductivity, the highest carrier mobility, and a maximum effective mass) teraFETs have a remarkably low essential resonant mobility, a greater DC voltage response than other teraFETs, and the ability to operate in the resonant mode in the sub-terahertz frequency range. On the other hand , the 2D hydrodynamic model (HDM) has been used in many works like [30,45-51] to increase model accuracy by accounting for 2D effects on the rectification.

Knap et al. [45] showed that the photoresponse both below and above the threshold gate voltage could be developed using this model by taking into account the gate leakage current that caused the detector response to be dampened in the sub-threshold region. As a result, the photoresponse reached a non-resonant maximum (see **Error! Reference source not found.**). However, the photoresponse can have sharp resonant peaks in the vicinity of plasma resonance [46,50] (see **Error! Reference source not found.**) and is non-quadratic at large input signals according to the work of Gutin et al.[51]. The hydrodynamic equations are used to describe the plasma waves in the 2D electron layer and the response of the channel in many regions of operation has been applied in many works such as Gorbenko et al.[46, 50,52] and Aizin [53]. They used standard hydrodynamic equations to describe the plasma waves in the 2D electron layer. Gorbenko et al.[46,52] demonstrated that the intrinsic FET channel exhibits a helicity-driven response in this region by applying the same principle to the study of the resonant regime of TeraFETs operation.

However, to account for the collisions with phonons and impurities, Aizin [53] presumptively used a ballistic electron transport model. The excess carrier concentration in the channel of TeraFETs that is created by the photoexcitation was studied [34, 54-56] by using 2D HDM. In these works, they used a 2D hydrodynamic approach to describe the excess carrier concentration generated by the laser photoexcitation.

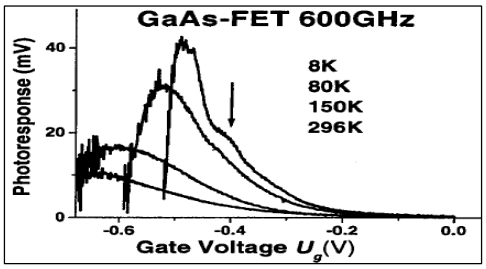

Fig. 2. The GaAs/AlGaAs 0.15 mm FET's photoresponse to radiation at 600 GHz at temperatures of 8, 80, 150, and 296 K. The maximum indicated by the arrow is the resonant detection seen at the coldest temperature: 8 K [45].

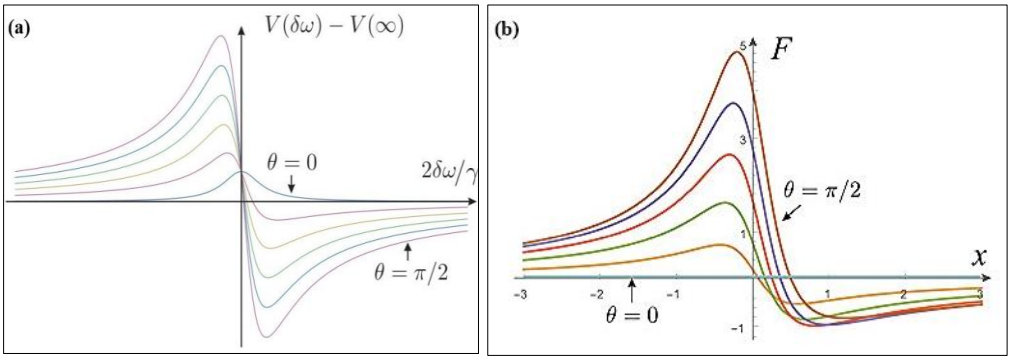

Fig. 3. Resonant dependence of a) the voltage response at a given frequency[46] and b) the basic plasmonic frequency's dimensionless response to radiation at various phase shifts [50].

Zhang et al. [57] described the behaviour of the electrons in the transistor channel and found that quantum effects must be taken into consideration to characterise the propagation of THz waves along the channel in teraFETs. Therefore, the Quantum Hydrodynamic Model (QHM) was used to support their analysis of the quantum effects.

$$\partial v/\partial t + v\,\partial v/\partial x + v/\tau = \frac{\hbar^2}{2m^2}\frac{\partial}{\partial x}\left(\frac{1}{\sqrt{n}}-\frac{\partial^2\sqrt{n}}{\partial^2 x}\right) - \frac{e}{m}\frac{\partial V_g}{\partial x} - \frac{1}{mn}\frac{\partial P}{\partial x} \quad (7)$$

where P is the local pressure in the 2D electron fluid. Finally, the HDM has proven to be effective in many studies for simulating some new device designs [20, 42, 58, 59] (**Error! Reference source not found.**). One of the studies that have used the hydrodynamic equation within TCAD simulators is the work of Delgado-Notario et al. [40]. They used this model to examine the electrical characteristics of deep-submicron FET transistors used in THz detection, and they used 2D HDM to achieve the photovoltaic THz response of strained-Si MODFETs at different gate lengths [58] by using the TCAD simulator. The structure of the device at different gate lengths is shown in **Fig. 5**. TCAD results obtained using HDM model physics have proven to be consistent with the experimental ones.

Si MOSFET TeraFETs were also simulated using TCAD simulators[11] Therefore, a suitable device design is required to maximize the PV response by optimizing the device's variables (such as its gate length). Ritesh Jain et al. [60] used time domain TCAD simulations to extract the effects of device parasitics (such as source resistance, drain resistance, and drain-to-body and channel-to-body capacitances) on the operation of CMOS FET THz detectors. It was found that by reducing the drain-to-body and channel-to-body capacitances and increasing the drain, and source resistances, the photoresponse can be improved.

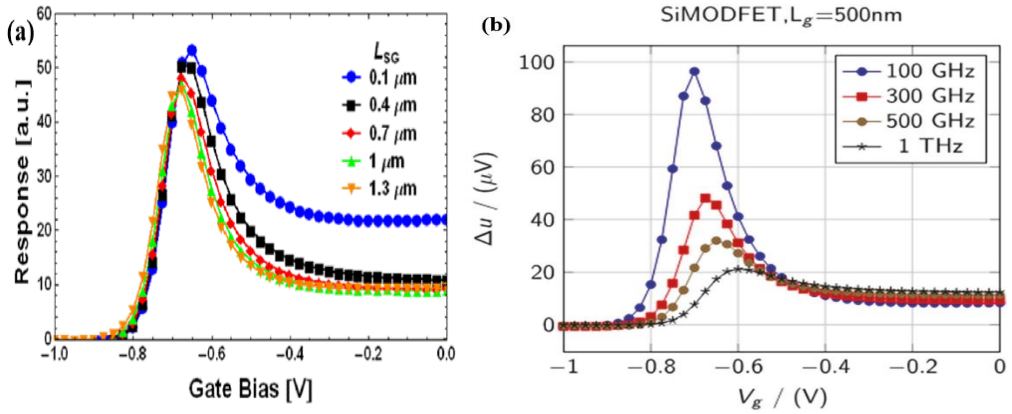

Fig. 4. Si MODFET photoresponse as a function of gate voltage with (a) different gate lengths under THz excitation of 300GHz [58](b) various frequency excitation (100, 300, 500 GHz, and 1 THz) for a device with Lg = 50nm[59].

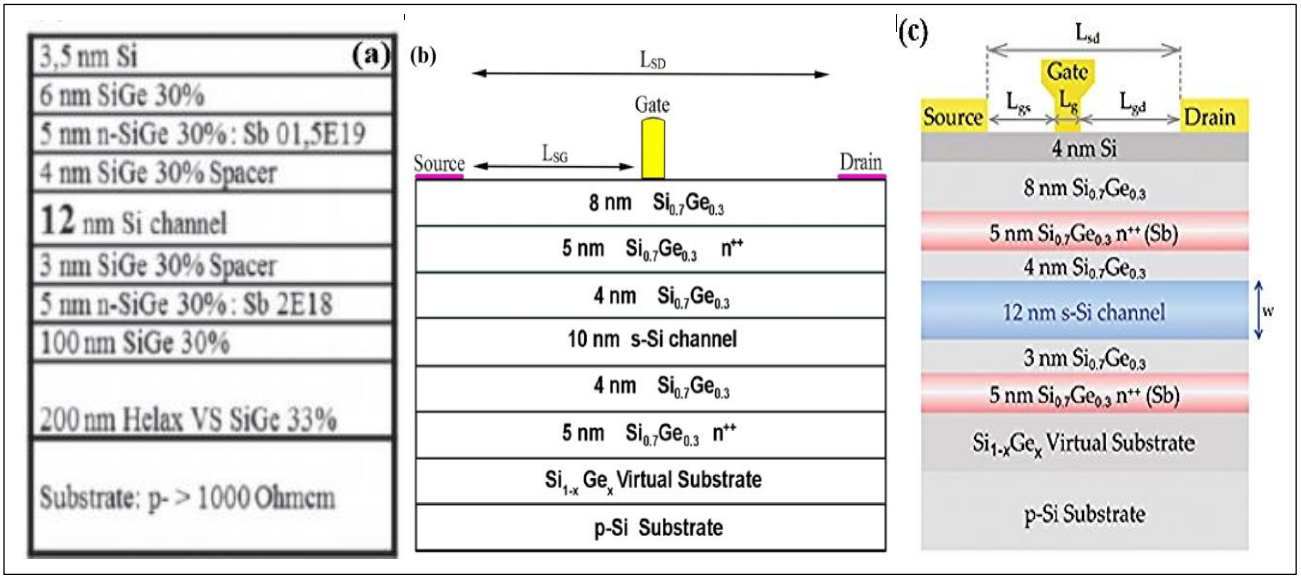

Fig. 5. The structure of Si/SiGe MODFET devices [42, 58, 59].

Raj [61] simulated the symmetrical design of a double gate dielectric modulated junctionless tunnel field-effect transistor (DG-DM-JLTFET)-based

structure (see **Fig. 6**). Using TCAD simulation, they extracted the sensitivity of the DG-DM-JLTFET to identify biomolecules by varying the drain current, subthreshold slope, and ION/IOFF ratio. HDM's main strength is in its use within the TCAD simulator. However, its complexity offers little insight into the physical operation of the FET.

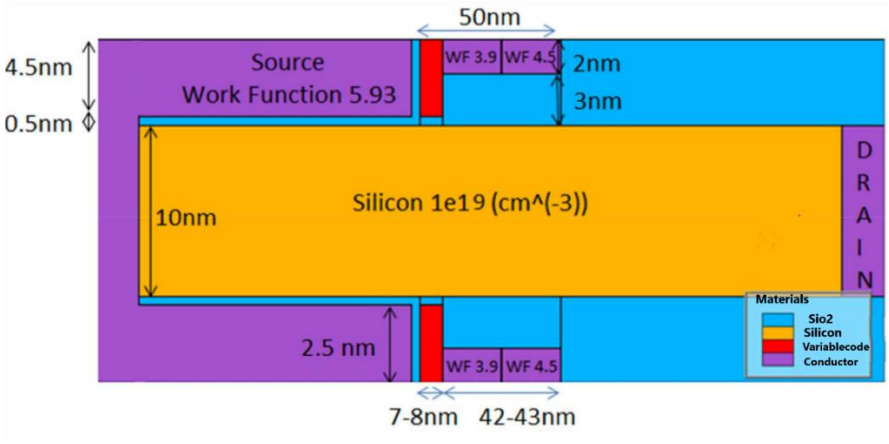

Fig. 6. Cross-sectional device structure of DG-DM-JLTFET [61].

2.3. Boltzmann Transport Model

Boltzmann transport-based models describe the nonlinear FET responsivity beyond cut-off by solving a set of differential wave equations like the hydrodynamic FET model. However, the Boltzmann transport-based models have the advantage of directly addressing each of the different phenomena that affect the output response. This has proven essential when device design modifications are required for higher responsivity. The Boltzmann transport model (drift transport model) was used to extract the response of teraFETs in multiple works along with the continuity equation. The teraFET in this approach can be described without the need to add any assumptions regarding charge density as in the above models. This approach also accounts for the different operation domains of the transistor.

Many researchers used the Boltzmann transport model to study the transport of electrons in the FET channel in different operation regions [22, 62]. Ibrahim et al. [22] used the semi-classical drift current equation to model the FET channel's electron transport in both linear and saturation regions. In this work, the channel was divided into two regions depending on the operation conditions: the linear part, where the gradual channel approximation (GCA) is applied, and the saturation region, where the GCA is not valid. When the transistor is in saturation, the separation between the two regions occurs at X_s, which is the saturation point where the onset of either pinch-off or saturation occurs.

In the linear region ($0<x<X_s$), the carrier velocity is linearly proportional to the electric field, while at the saturation region ($X_s<x<L_g$), the response saturates at a constant value in the saturation region. In the saturation region, the total change in dc potential due to ac applied signal (ΔV_{sat}) can be expressed as

$$\Delta V_{sat} = V_{sat}(L_g\text{-}X_s)\text{-}\, V_{sat}(L_g\text{-}X_s^{*}) \tag{8}$$

This means that rectification in the linear region changes the length of the saturation region, and consequently, the amplification factor applied to that region. Furthermore, Ibrahim et al. [22] divided the saturation regime into three sub-regimes (complete, deep, and shallow saturation) using the drift FET model, each of which has a unique rectification response function. This work also studied the relation between the decay length of the AC signal and the saturation length of the channel, which led to the distinction between shallow and deep saturation.

Based on the Boltzmann transport model, the principal characteristics of a GaN HEMT's THz response (see **Error! Reference source not found.**) are described in the work of Hou et al. [62], and the rectified second-order output signal is also extracted. According to equation (9), the first term is an indication of a perturbation along the channel direction, and the second term is an indication of a perturbation along the gate direction.

$$\begin{cases} \delta\tilde{V}_{ds} = \delta V_{ds}\, cos(\omega) \\ \delta\tilde{V}_{g} = \delta V_{g}\, cos(\omega + \phi) \end{cases} \Rightarrow \begin{cases} V_{ds} \longrightarrow V_{ds} + \delta\tilde{V}_{ds} \\ V_{g} \longrightarrow V_{g} + \delta\tilde{V}_{g} \end{cases} , i_{ds}\, G_o(V_g) V_{ds} \tag{9}$$

Also, by using the Boltzmann transport model, Hassanalieragh et al. [21] have shown that the sub-threshold Si MOSFETs' exponential dependence of the channel electron density on the gate-source voltage is the effective nonlinear mechanism. Two modes of detection are possible by because the electron densities on the source and drain sides of the channel differ, if the asymmetry is maintained. Accordingly, the diffusion current was shown to be.

$$j_{diff} = D_e(n_e(S)\ - n_e(D)/\mathrm{Lg}) \qquad \text{Open drain (photovoltaic)} \tag{10}$$

$$i_{diff} = W \int_0^{Y_{ch}} j_{diff}\, dy \qquad \text{Current flow (photoconductive)} \tag{11}$$

Where j_{diff} is the diffusion current density, D_e is the electron diffusion constant, W is the gate width, $n_e(S)$, and $n_e(D)$ is electron density at the source and drain sides of the channel, respectively, and Y_{ch} is the channel depth.

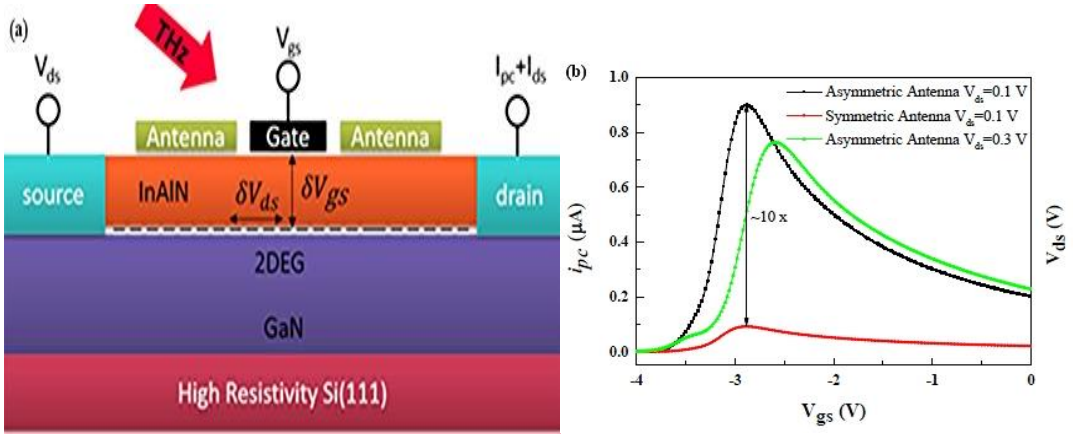

Fig. 7. (a) The cross-section of the GaN HEMT detector. (b) The photocurrent vs Vg for both the conventionally designed symmetric antenna and the suggested asymmetric antenna [62].

The 2D photovoltaic detector (shown in

Fig. 7(a)) is simulated in the time domain using the Synopsis device simulator (Sentaurus) and is used to confirm the above assumption. The authors used the device simulation results to verify their proposed THz detection theory (see

Fig. 8 (b)). From the above-mentioned review, Boltzmann transport based NQS models present a significant approach for physics-based models of teraFETs. These models can be directly related to the device's design as well as operation. Such a feature is important as it gives researchers insight into how to develop devices with a higher response.

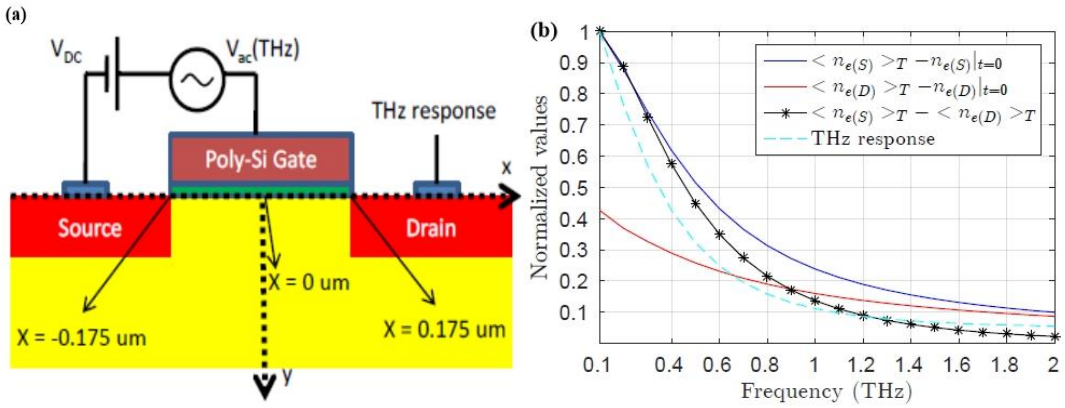

Fig. 8. (a) Si MOSFET in photovoltaic THz detection mode created by Sentaurus device simulator. (b)The values of the DC shift in electron density at the channel's source and drain sides are normalized to the maximum DC shift there. Moreover, the THz response and the variations in the two DC shifts [14].

2.4. Equivalent Circuit Model

The equivalent circuit model uses the superposition method to represent the NQS relationship between the FET's characteristics by representing the channel as a transmission line circuit (TLC). In the TLC approach, the FET channel can be modelled as a distributed RC or RLC network circuit. These distributed RC or RLC network elements (channel resistance and capacitors between the gate and the channel points) make the equivalent circuit model another form of the Boltzmann transport model. The Boltzmann transport model has been used in numerous studies, and it has been demonstrated that the circuit configuration is directly related to the potential and current boundary conditions.

Using this approach, the effect of parasitic elements of extrinsic FET was the focus of both Son and Yang [63] and Kopyt [64] (**Fig. 9** and **Fig. 10**). Kopyt et al. [64] used the transmission line method to create a model of the MOSFET's channel to study the behaviour of the detector under sub-THz radiation delivered through the gate and source pads. By representing the device with an electric equivalent circuit (as in the TCL model), the device could be simulated using a standard circuit simulator (SPICE model) at frequencies significantly higher than the device cut-off frequency, as in the work of Guttin et al. [25, 65, 66].

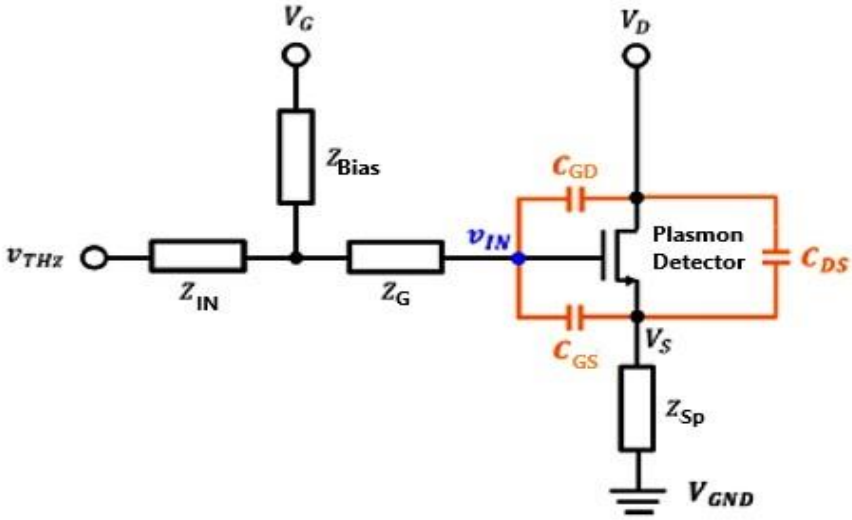

Fig. 9. Basic model for the TeraFET detector at high frequency including the parasitic capacitances [63].

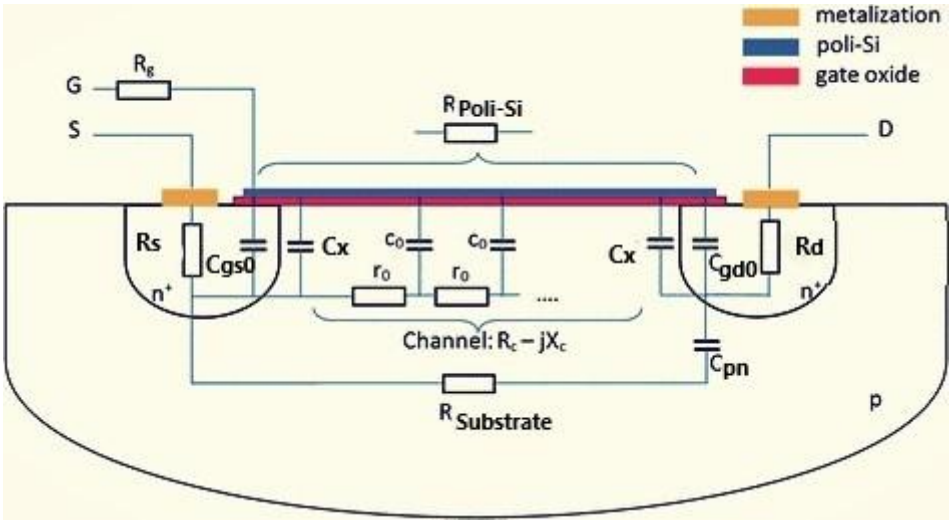

Fig. 10. The construction of an n-MOSFET on a p-type well with two ohmic contacts for the drain and source and a polysilicon gate on a narrow gate oxide is simplified [64].

This model is also compared to traditional SPICE models (**Fig. 11 a,b**) which fail to model the device operated in Quasi Stationary (QS) conditions, but for Non-Quasi-Stationary (NQS) conditions, the SPICE circuit model of a THz FET response is appropriated [24, 67– 69].

Whereas the channel can be represented by a transmission line model with nonlinear distributed elements [24, 61]. *Elkhatib et al.* [68] show the multi-segment SPICE model (see **Fig. 12**), which is based on the unified charge control model (UCCM), the distributed nonlinear impedances, and the internal capacitances of the intrinsic FETs.

It is worth noting that the results of Ayoub et al. [67] have shown that the channel has little effect on the rectification process. and the transmission line circuit (TLC) boundary elements (**Fig. 13**) at the source/drain contacts are the principal source for the second order response that had the maximum rectification response. This result is shared by the work of Ludwig et al. [70], who used the Fermi energy continuity equation to extract the equivalent circuit model elements.

The previous approaches fall between the hydrodynamic-based TCAD simulation and the Boltzmann transport-based model. On one side, it lends itself well to circuit simulators, while on the other, the values of the circuit elements are extracted from the Boltzmann transport model and are hence physics based with explicit dependence on the design and operation.

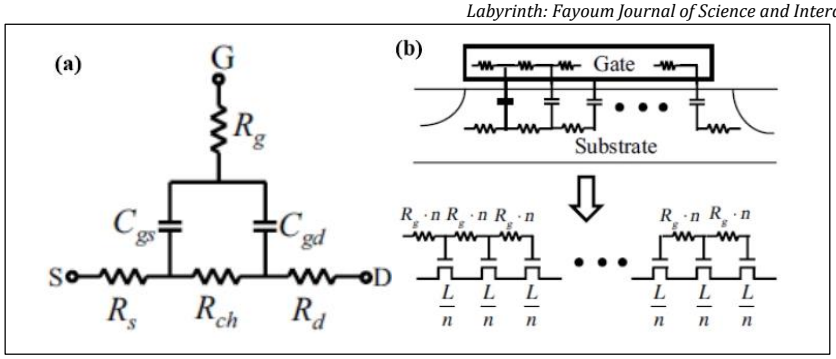

Fig. 11. (a) Typical FET circuit representation in SPICE (b)THz SPICE model with n gate length segments L_g/n, interconnected gate resistance of R_g/n, distributed RC recognition of device channel, and equivalent SPICE model [25].

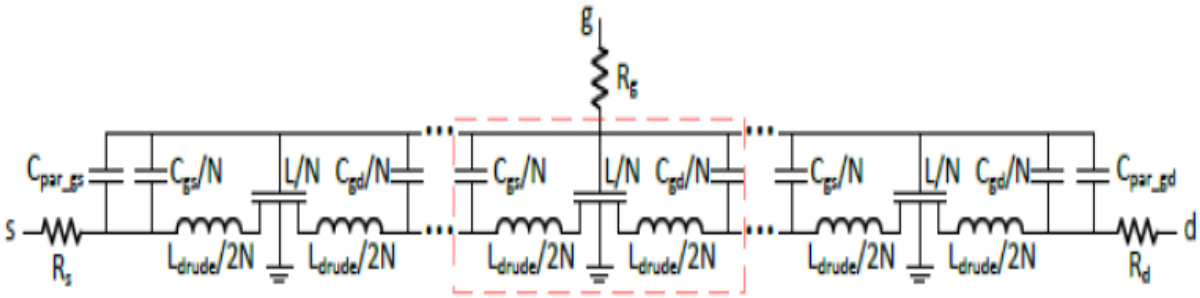

Fig. 12. Equivalent circuit of each section of the multi-segment SPICE model with leakage elements [68].

The different variations presented above are due to different approximations for the circuit elements considered by the researchers to be significant elements contributing to the nonlinear rectification process. A comparative study of the relative weight of the contributions to each has not been presented yet.

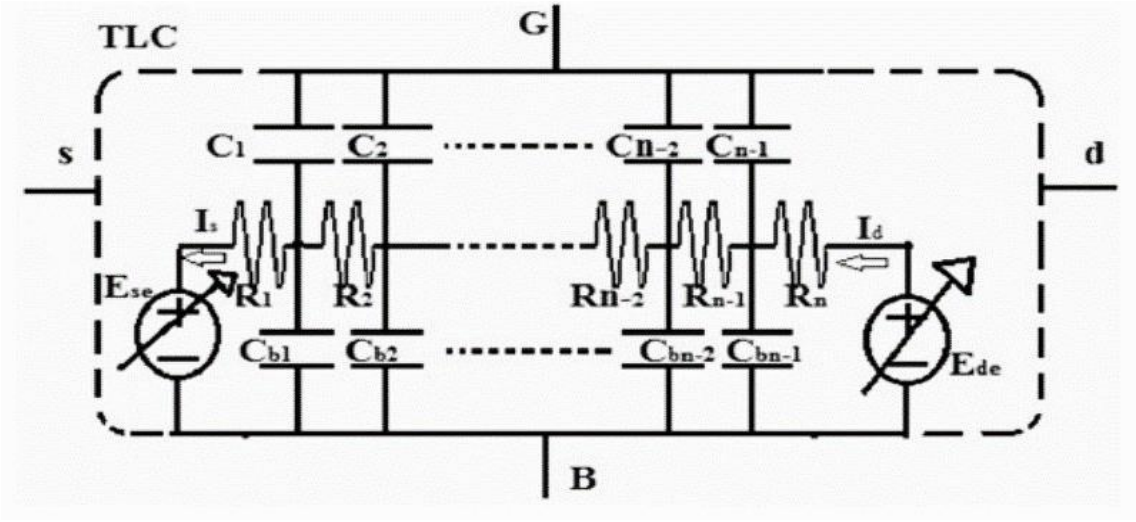

Fig. 13. The channel of the circuit for the bundled N-element R-C transmission line (TLC) [67].

2.5. Phenomenological Model

A few phenomenological models were developed to describe the FET THz rectification in terms of the device output characteristics [26], [71]–[73] as in the work of Sakowicz et al. [26], where they found that under broadband operation conditions, the phenomenological model connects the photoresponse to the conductivity of the DC channel, which can be represented by various electronic models. But it did not cover the effect of source-drain current. Other models that have been used to describe the operation of a transistor in various channel systems include the work of Elkhatib et al. [72] and But et al. [73].

In the work of Elkhatib et al. [72], the authors described the response of InGaAs/GaAs HEMTs in the saturation and ohmic regimes. Their model in

the non-resonance detection case ($\omega\tau \ll 1$) showed that the AC voltage falls off exponentially along the channel on the typical spatial scale. Then they concluded that the response increases linearly in the deep saturation regime and increases greatly at the intermediate point between the linear and saturation regions. El Khatib et al. [73] described the transistor's operation at three different operation regions. These three regions are weak ($V_g << V_{Th}$), moderate ($V_g \approx V_{Th}$), and strong ($V_g >> V_{Th}$) inversion. It is possible to define the drain-source current (I_{DS}) by its diffusion component using the following equation:

$$I_{DS} = I_0 \times \left(1 - exp^{-\frac{V_D}{\phi_t}}\right) \times exp^{-\frac{V_g - V_{Th}}{\eta\phi_t}} \quad (12)$$

where I_0 is the current factor, V_D is the drain voltage, ϕ_t is the thermal voltage, and η is the ideality factor of the FET. The work of Földesy [74] took into account the impact of bulk potential and used the phenomenological representation to identify the long channel FET detector behaviour in all FET operating domains, including depletion, strong and weak inversion, and non-zero source-drain current. With the help of the drain current ratio (g_m/I_{DS}), this model connects the photoresponse to the gate transconductance. He started with the response ΔV, which is determined by the channel conductivity (σ_s) and the small current DC transfer function to get.

$$\Delta V \propto P_{ac} \frac{\partial}{\partial V_g} ln\ ln\ (\sigma_s) \propto P_{ac} \frac{\partial}{\partial V_g} ln\ ln\left[I_{DS}(V_{gs})\right] \quad (13)$$

and

$$\frac{\partial}{\partial V_g} ln\ ln\left[I_{DS}(V_{gs})\right] = \frac{1}{I_{DS}(V_{gs})} \frac{\partial I_{DS}(V_{gs})}{\partial V_g} = \frac{g_m}{I_{DS}(V_{gs})} \quad (14)$$

where P_{ac} is the incident RF power. From these equations, he concluded that the maximum g_m/I_m ratio appeared in weak inversion and was equivalent to $1/n\ V_{the}$ (where n is the inclination factor and $V_{the}$is the thermal voltage), and with source-drain current lowering exponentially in the reduced gate-source voltage region, the g_m/I_m quickly decreases as leakage currents take over in I_{DS}[74].

3. Modelling the Effects of Boundary Conditions

While most of the research literature assumed coupling of the incident radiation or AC signal to a single contact point (usually gate or source), it was obvious from the beginning that it could directly couple to all the FET contacts. Experimental observations emphasised the influence of the coupling to the contacts of the FET when it was observed that a symmetrically designed FET suffers a strong reduction in the output response. On the contrary, the reduction was negligible when the FET was operated in the current flow condition. This is because the electrical coupling of the source and drain contacts would cause strong suppression of the drain signal. Some authors have resorted to designing an asymmetrical device through geometric design to consistently induce symmetry. The effect of asymmetry was further investigated in the case of broadband detection, as in the work of Ibrahim et al. [69].

$$\delta P_1 = (\eta_{gs1}^p - \eta_{gd1}^p H)\ V_{gs1}^{E2} \quad (15)$$

where δP_1 is the difference between the squared amplitude of the input AC signal at the gate/source port and gate/drain port, η_{gs1}^p and η_{gd1}^p refer to the potential coupling efficiency at the gate/source port and gate/drain port, respectively, V_{gs1}^{E2} is the extrinsic AC signal at the gate/source port, and H is the ratio of the two source signals that are applied to the input ports. The coupling circuit for each AC input signal (gate/source and gate/drain) is illustrated in **Fig. 14**. As a result, there are now five sources of asymmetry in the model: feed-induced, physically-induced, current-induced, frequency-induced, and phase-induced asymmetry.

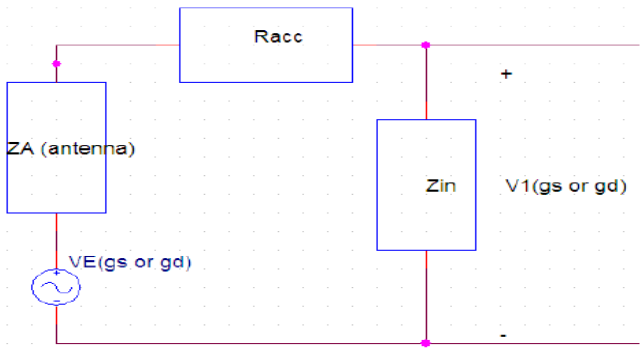

Fig. 14. Circuit diagram for the external FET's input AC signal coupling [69].

Gorbenko et al. [41] developed the effect of phase asymmetry according to the plasma wave theory by coupling THz radiation to the FET channel using two antennas located on opposing sides with a phase shift (θ) between them (**Fig. 15**). This phase shift, which affects the boundary conditions for the electron fluid in the transistor channel, results in asymmetry. This phase-induced asymmetry approach eliminates the issues caused by frequency-dependent input, output, and load impedances by using the same antennas at the source and drain of the FET detector, making it much simpler to manage.

$$X=\begin{cases} V(x=0)=V_g+V_a\,cos(\omega t) \\ V(x=Lg)=V_g+V_a\,cos(\omega t+\theta) \end{cases} \quad (16)$$

Where $V_s(x=0)$ and $V_d(x=Lg)$ are the voltages at the channel's source and drain, respectively.

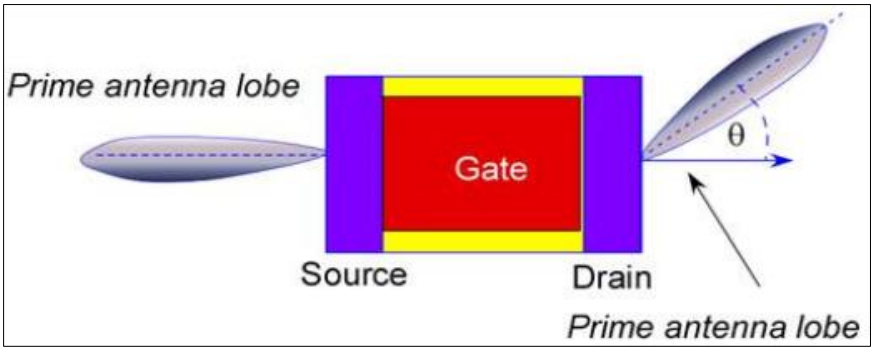

Fig. 15. Operating principles for the phase shift caused by asymmetric antennas and circularly polarized radiation in the TeraFET Spectrometer [41].

Finally, these mentioned models explain the behaviour of FET under the effect of THz radiation by using the continuity equation and another transport model equation. All of them are interested in the FET's channel as an active rectifying element for operation beyond cut-off in terahertz detectors. They also consider the DC second-order terms (which appear at high frequencies) neglected in the device literature.

4. Conclusions

Recently, TeraFETs have shown themselves to be effective alternatives for highly sensitive THz detectors. So studying the physical models that are used in modelling the FET as THz detectors is a target of experimental and theoretical studies. Accordingly, the theoretical models (such as hydrodynamic, plasmonic, and phenomenological models) used to study the response of TeraFET detectors were reviewed in this work to reach a better understanding of the physical phenomena guiding the operation of the FET in THz detection. These models explain the behaviour of FET under the effect of THz radiation by using the continuity equation and other transport model equations. All of them are interested in the FET's channel as an active rectifying element for operation beyond cut-off in terahertz detectors. They also consider the DC second-order terms (at high frequencies), which are neglected in conventional device models. Finally, the advantages of the mentioned models and the comparison among them help us optimise devices' designs to reach the best performance of FETs in THz detection.

Acknowledgment

The authors would like to thank Fayoum University for supporting the publication of this work.

Author Contributions

All authors contributed to this work. Both Y. Mohamed and N. Ibrahim followed the revision and submission of the manuscript for publication.

Declaration of Competing Interest

The authors declare that they do not have any competing interests.

References

[1] Q. Meng, Q. Lin, F. Han, W. Jing, Y. Wang, and Z. Jiang, "A Terahertz Detector Based on Double-Channel GaN/AlGaN High Electronic Mobility Transistor," *Materials*, p. 11, 2021.
[2] R. A. Lewis, "A review of terahertz sources," *J. Phys. Appl. Phys.*, vol. 47, no. 37, p. 374001, Sep. 2014, doi: 10.1088/0022-3727/47/37/374001.

[3] P. L. Richards, "Bolometers for infrared and millimeter waves," *J. Appl. Phys.*, vol. 76, no. 1, pp. 1–24, Jul. 1994, doi: 10.1063/1.357128.
[4] J. Glenn *et al.*, "Current status of Bolocam: a large-format millimeter-wave bolometer camera," presented at the Astronomical Telescopes and Instrumentation, T. G. Phillips and J. Zmuidzinas, Eds., Waikoloa, Hawai'i, United States, Feb. 2003, p. 30. doi: 10.1117/12.459369.
[5] S. Ariyoshi *et al.*, "Terahertz imaging with a direct detector based on superconducting tunnel junctions," *Appl. Phys. Lett.*, vol. 88, pp. 203503–203503, May 2006, doi: 10.1063/1.2204842.
[6] A. Lisauskas *et al.*, "Exploration of terahertz imaging with silicon MOSFETs," *J. Infrared Millim. Terahertz Waves*, vol. 35, no. 1, pp. 63–80, 2014.
[7] W. Knap *et al.*, "Terahertz emission by plasma waves in 60 nm gate high electron mobility transistors," *Appl. Phys. Lett.*, vol. 84, no. 13, pp. 2331–2333, 2004.
[8] N. Ibrahim, N. H. Rafat, and S. El-Din Elnahwy, "Simulation study for the use of transistor contacts for sub-terahertz radiation detection," *IET Microw. Antennas Propag.*, vol. 10, no. 7, pp. 784–790, May 2016, doi: 10.1049/iet-map.2015.0492.
[9] S. Sankaran and K. K. O, "Schottky barrier diodes for millimeter wave detection in a foundry CMOS process," *IEEE Electron Device Lett.*, vol. 26, no. 7, pp. 492–494, Jul. 2005, doi: 10.1109/LED.2005.851127.
[10] Y. Liu, J. Sun, L. Tong, Y. Li, and T. Deng, "High-performance one-dimensional MOSFET array photodetectors in the 0.8-μm standard CMOS process," *Opt. Express*, vol. 30, no. 24, pp. 43706–43717, Nov. 2022, doi: 10.1364/OE.475687.
[11] Y. A. Mohamed, N. Y. Ibrahim, M. Y. F. El Zayat, and S. E. A. Elnahwy, "Modeling and simulation of short channel length effect in open drain MOSFET THz detectors," *J. Eng. Appl. Sci.*, vol. 70, no. 1, p. 37, May 2023, doi: 10.1186/s44147-023-00195-8.
[12] G. J. Fertig, "Evaluation of MOSFETs for Terahertz Detector Arrays," *Rochester Inst. Technol. Clemson Univ.*, p. 188, 2014.
[13] H. Emami-Nejad, A. Mir, Z. Lorestaniweiss, A. Farmani, and R. Talebzadeh, "First designing of a silicene-based optical MOSFET with outstanding performance," *Sci. Rep.*, vol. 13, no. 1, p. 6563, Apr. 2023, doi: 10.1038/s41598-023-33620-2.
[14] N. Shabanzadeh *et al.*, "A Study of the Effects Limiting the Responsivity of A Broadband THz Power Detector with On-chip Antenna in 0.13μm SiGe HBT Technology".
[15] H. M. Abdelbaset, T. A. Elkhatib, N. Y. Ibrahim, and N. H. Rafat, "THz Detection by HBT Justified by Nonlinear Analytical Modeling and TCAD Simulation," SSRN, preprint, 2023. doi: 10.2139/ssrn.4368150.
[16] W. Knap, Y. Deng, S. Rumyantsev, and M. S. Shur, "Resonant detection of subterahertz and terahertz radiation by plasma waves in submicron field-effect transistors," *Appl. Phys. Lett.*, vol. 81, no. 24, pp. 4637–4639, Dec. 2002, doi: 10.1063/1.1525851.
[17] A. R. Arehart *et al.*, "Next generation defect characterization in nitride HEMTs," *Phys. Status Solidi C*, vol. 8, no. 7–8, pp. 2242–2244, Jul. 2011, doi: 10.1002/pssc.201000955.
[18] G. Paz-Martínez *et al.*, "Temperature and Gate-Length Dependence of Subthreshold RF Detection in GaN HEMTs," *Sensors*, vol. 22, no. 4, p. 1515, Feb. 2022, doi: 10.3390/s22041515.
[19] X. G. Peralta *et al.*, "Terahertz photoconductivity and plasmon modes in double-quantum-well field-effect transistors," *Appl. Phys. Lett.*, vol. 81, no. 9, pp. 1627–1629, Aug. 2002, doi: 10.1063/1.1497433.
[20] M. Dyakonov and M. Shur, "Shallow water analogy for a ballistic field effect transistor: New mechanism of plasma wave generation by dc current," *Phys. Rev. Lett.*, vol. 71, no. 15, pp. 2465–2468, Oct. 1993, doi: 10.1103/PhysRevLett.71.2465.
[21] M. Hassanalieragh, J. D. Newman, K. Fourspring, and Z. Ignjatovic, "THz detection in sub-threshold Si MOSFETs by non-linear channel electron density modulation," in *2017 IEEE 60th International Midwest Symposium on Circuits and Systems (MWSCAS)*, Boston, MA, USA: IEEE, Aug. 2017, pp. 1434–1437. doi: 10.1109/MWSCAS.2017.8053202.
[22] N. Y. Ibrahim, N. H. Rafat, and S. E. A. Elnahwy, "Drift transport model of field effect transistors in saturation beyond cutoff," *J. Phys. Appl. Phys.*, vol. 48, no. 13, p. 135102, Apr. 2015, doi: 10.1088/0022-3727/48/13/135102.
[23] I. Chamas, "A NEW NON-QUASI STATIC MOSFET MODEL," *Univ. Pittsburgh*, p. 127, 2005.
[24] N. Y. Ibrahim, N. H. Rafat, and S. E. A. Elnahwy, "Modeling of Field Effect Transistor Channel as a Nonlinear Transmission Line for Terahertz Detection," *J. Infrared Millim. Terahertz Waves*, vol. 34, no. 10, pp. 606–616, Oct. 2013, doi: 10.1007/s10762-013-0009-0.
[25] A. Gutin, T. Ytterdal, V. Kachorovskii, A. Muraviev, and M. Shur, "THz SPICE for Modeling Detectors and Nonquadratic Response at Large Input Signal," *IEEE Sens. J.*, vol. 13, no. 1, p. 9, 2013.
[26] M. Sakowicz *et al.*, "Terahertz responsivity of field effect transistors versus their static channel conductivity and loading effects," *J. Appl. Phys.*, vol. 110, no. 5, p. 054512, Sep. 2011, doi: 10.1063/1.3632058.
[27] J. A. Delgado-Notario, V. Clericò, K. Fobelets, J. E. Velázquez-Pérez, and Y. M. Meziani, "Room-Temperature Terahertz Detection and Imaging by Using Strained-Silicon MODFETs," in *Design, Simulation and Construction of Field Effect Transistors*, D. Vikraman and H.-S. Kim, Eds., InTech, 2018. doi: 10.5772/intechopen.76290.
[28] M. I. Dyakonov and M. S. Shur, "Plasma wave electronics: novel terahertz devices using two dimensional electron fluid," *IEEE Trans. Electron Devices*, vol. 43, no. 10, pp. 1640–1645, Oct. 1996, doi: 10.1109/16.536809.
[29] M. Dyakonov and M. S. Shur, "Plasma Wave Electronics for Terahertz Applications," in *Terahertz Sources and Systems*, R. E. Miles, P. Harrison, and D. Lippens, Eds., in NATO Science Series. Dordrecht: Springer Netherlands, 2001, pp. 187–207. doi: 10.1007/978-94-010-0824-2_12.
[30] M. Dyakonov and M. Shur, "Detection, mixing, and frequency multiplication of terahertz radiation by two-dimensional electronic fluid," *IEEE Trans. Electron Devices*, vol. 43, no. 3, pp. 380–387, Mar. 1996, doi: 10.1109/16.485650.
[31] Y.M. Meziani *et al.*, "Detection of Terahertz Radiation from Submicron Plasma Waves Transistors," in *Bolometers*, U. Perera, Ed., InTech, 2012. doi: 10.5772/34562.
[32] D. Veksler, F. Teppe, A. P. Dmitriev, V. Yu. Kachorovskii, W. Knap, and M. S. Shur, "Detection of terahertz radiation in gated two-dimensional structures governed by dc current," *Phys. Rev. B*, vol. 73, no. 12, p. 125328, Mar. 2006, doi: 10.1103/PhysRevB.73.125328.
[33] F. Palma, "Self-Mixing Model of Terahertz Rectification in a Metal Oxide Semiconductor Capacitance," *Electronics*, vol. 9, no. 3, p. 479, Mar. 2020, doi: 10.3390/electronics9030479.
[34] A. Mahi, C. Palermo, H. Marinchio, A. Belgachi, and L. Varani, "Saturation of THz detection in InGaAs-based HEMTs: a numerical analysis," *Phys. B Condens. Matter*, vol. 500, pp. 1–3, Nov. 2016, doi: 10.1016/j.physb.2016.07.024.
[35] X. Liu, "NUMERICAL AND COMPACT FIELD EFFECT TRANSISTOR MODELS VALIDATED FOR TERAHERTZ DETECTION," *Rensselaer Polytech. Inst.*, p. 24, 2019.
[36] H.-T. Chen *et al.*, "Electronic control of extraordinary terahertz transmission through subwavelength metal hole arrays," *Opt. Express*, vol. 16, no. 11, pp. 7641–7648, 2008.
[37] V. V. Popov, D. V. Fateev, T. Otsuji, Y. M. Meziani, D. Coquillat, and W. Knap, "Plasmonic terahertz detection by a double-grating-gate field-effect transistor structure with an asymmetric unit cell," *Appl. Phys. Lett.*, vol. 99, no. 24, p. 243504, Dec. 2011, doi: 10.1063/1.3670321.
[38] Y. Zhang and M. Shur, "THz detection and amplification using plasmonic field effect transistors driven by DC drain currents," *J. Appl. Phys.*, vol. 132, no. 19, p. 193102, Nov. 2022, doi: 10.1063/5.0128496.
[39] Y. Zhang and M. S. Shur, "Resonant THz detection by periodic multi-gate plasmonic FETs".
[40] J. Delgado-Notario, J. Velazquez-Perez, Y. Meziani, and K. Fobelets, "Sub-THz Imaging Using Non-Resonant HEMT Detectors," *Sensors*, vol. 18, no. 2,

p. 543, Feb. 2018, doi: 10.3390/s18020543.
[41] M. W. Ryu, J. S. Lee, K. Park, K. R. Kim, W.-K. Park, and S.-T. Han, "TCAD modeling and simulation of non-resonant plasmonic THz detector based on asymmetric silicon MOSFETs," in *2013 International Conference on Simulation of Semiconductor Processes and Devices (SISPAD)*, Glasgow, United Kingdom: IEEE, Sep. 2013, pp. 200–203. doi: 10.1109/SISPAD.2013.6650609.
[42] J. A. Delgado Notario *et al.*, "Experimental and theoretical studies of Sub-THz detection using strained-Si FETs," *J. Phys. Conf. Ser.*, vol. 906, p. 012003, Oct. 2017, doi: 10.1088/1742-6596/906/1/012003.
[43] Y. Zhang and M. S. Shur, "Ultrashort Pulse Detection and Response Time Analysis Using Plasma-Wave Terahertz Field-Effect Transistors," *IEEE Trans. Electron Devices*, vol. 68, no. 2, pp. 903–910, Feb. 2021, doi: 10.1109/TED.2020.3043992.
[44] Y. Zhang and M. S. Shur, "p-Diamond, Si, GaN, and InGaAs TeraFETs," *IEEE Trans. Electron Devices*, vol. 67, no. 11, pp. 4858–4865, Nov. 2020, doi: 10.1109/TED.2020.3027530.
[45] W. Knap *et al.*, "Nonresonant detection of terahertz radiation in field effect transistors," *J. Appl. Phys.*, vol. 91, no. 11, pp. 9346–9353, Jun. 2002, doi: 10.1063/1.1468257.
[46] I. V. Gorbenko, V. Y. Kachorovsky, and M. S. Shur, "Plasmonic polarization-sensitive detector of terahertz radiation," *J. Phys. Conf. Ser.*, vol. 1236, no. 1, p. 012029, Jun. 2019, doi: 10.1088/1742-6596/1236/1/012029.
[47] V. Ryzhii, M. Ryzhii, M. S. Shur, V. Mitin, A. Satou, and T. Otsuji, "Resonant plasmonic terahertz detection in graphene split-gate field-effect transistors with lateral p-n junctions," *J. Phys. Appl. Phys.*, vol. 49, no. 31, p. 315103, Aug. 2016, doi: 10.1088/0022-3727/49/31/315103.
[48] M. I. Dyakonov, "Generation and detection of Terahertz radiation by field effect transistors," *Comptes Rendus Phys.*, vol. 11, no. 7–8, pp. 413–420, Aug. 2010, doi: 10.1016/j.crhy.2010.05.003.
[49] B. Jamali and A. Babakhani, "A Fully Integrated 50–280-GHz Frequency Comb Detector for Coherent Broadband Sensing," *IEEE Trans. Terahertz Sci. Technol.*, vol. 9, no. 6, pp. 613–623, Nov. 2019, doi: 10.1109/TTHZ.2019.2944129.
[50] I. V. Gorbenko, V. Y. Kachorovskii, and M. Shur, "Terahertz plasmonic detector controlled by phase asymmetry," *Opt. Express*, vol. 27, no. 4, p. 4004, Feb. 2019, doi: 10.1364/OE.27.004004.
[51] A. Gutin, V. Kachorovskii, A. Muraviev, and M. Shur, "Plasmonic terahertz detector response at high intensities," *J. Appl. Phys.*, vol. 112, no. 1, p. 014508, Jul. 2012, doi: 10.1063/1.4732138.
[52] I. V. Gorbenko, V. Yu. Kachorovskii, and M. S. Shur, "Plasmonic Helicity-Driven Detector of Terahertz Radiation," *Phys. Status Solidi RRL – Rapid Res. Lett.*, vol. 13, no. 3, p. 1800464, Mar. 2019, doi: 10.1002/pssr.201800464.
[53] G. R. Aizin, J. Mikalopas, and M. Shur, "Plasmonic instabilities in two-dimensional electron channels of variable width," *Phys. Rev. B*, vol. 101, no. 24, p. 245404, Jun. 2020, doi: 10.1103/PhysRevB.101.245404.
[54] H. Marinchio *et al.*, "Hydrodynamic modeling of optically excited terahertz plasma oscillations in nanometric field effect transistors," *Appl. Phys. Lett.*, vol. 94, no. 19, p. 192109, May 2009, doi: 10.1063/1.3137189.
[55] H. Marinchio *et al.*, "Experimental and theoretical investigation of terahertz optical-beating detection by plasma waves in high electron mobility transistors," *Phys. Status Solidi C*, vol. 5, no. 1, pp. 257–260, Jan. 2008, doi: 10.1002/pssc.200776572.
[56] J. Torres *et al.*, "Plasma Waves Subterahertz Optical Beating Detection and Enhancement in Long-Channel High-Electron-Mobility Transistors: Experiments and Modeling," *IEEE J. Sel. Top. Quantum Electron.*, vol. 14, no. 2, pp. 491–497, 2008, doi: 10.1109/JSTQE.2007.910988.
[57] L.-P. Zhang, C.-X. Liu, J.-X. Feng, and J.-Y. Su, "The effect of nonideal boundary condition on instability of THz plasma waves in quantum field-effect transistors," *AIP Adv.*, vol. 12, no. 3, p. 035143, Mar. 2022, doi: 10.1063/5.0083466.
[58] J. A. D. Notario, Y. M. Meziani, and J. E. Velázquez-Pérez, "TCAD study of sub-THz photovoltaic response of strained-Si MODFET," *J. Phys. Conf. Ser.*, vol. 647, p. 012041, Oct. 2015, doi: 10.1088/1742-6596/647/1/012041.
[59] J. A. Delgado Notario *et al.*, "Sub-Micron Gate Length Field Effect Transistors as Broad Band Detectors of Terahertz Radiation," *Int. J. High Speed Electron. Syst.*, vol. 25, no. 03n04, p. 1640020, Sep. 2016, doi: 10.1142/S0129156416400206.
[60] R. Jain, H. Rucker, and N. R. Mohapatra, "Optimization of Si MOS transistors for THz detection using TCAD simulation," in *2014 International Conference on Simulation of Semiconductor Processes and Devices (SISPAD)*, Yokohama, Japan: IEEE, Sep. 2014, pp. 213–216. doi: 10.1109/SISPAD.2014.6931601.
[61] G. Wadhwa and B. Raj, "Design, Simulation and Performance Analysis of JLTFET Biosensor for High Sensitivity," *IEEE Trans. Nanotechnol.*, vol. 18, pp. 567–574, 2019, doi: 10.1109/TNANO.2019.2918192.
[62] H. Hou, "Modelling of GaN HEMTs as Terahertz Detectors Based on Self-Mixing," *Procedia Eng.*, p. 5, 2016.
[63] J.-H. Son and J.-R. Yang, "Quasi-static Analysis Based on an Equivalent Circuit Model for a CMOS Terahertz Plasmon Detector in the Subthreshold Region," *Sensors*, p. 12, 2019.
[64] P. Kopyt, B. Salski, J. Marczewski, P. Zagrajek, and J. Lusakowski, "Parasitic Effects Affecting Responsivity of Sub-THz Radiation Detector Built of a MOSFET," *J. Infrared Millim. Terahertz Waves*, vol. 36, no. 11, pp. 1059–1075, Nov. 2015, doi: 10.1007/s10762-015-0188-y.
[65] A. Gutin, S. Nahar, M. Hella, and M. Shur, "Modeling Terahertz Plasmonic Si FETs With SPICE," *IEEE Trans. Terahertz Sci. Technol.*, vol. 3, no. 5, pp. 545–549, Sep. 2013, doi: 10.1109/TTHZ.2013.2262799.
[66] Hao Wu, Haipeng Fu, Fanyi Meng, and Kaixue Ma, "Responsivity enhancement techniques for CMOS source-driven terahertz detectors," Microw Opt Technol Lett. ;64:1036–1041 2022. https://onlinelibrary.wiley.com/doi/full/10.1002/mop.33241 (accessed May 16, 2023).
[67] A. B. Ayoub, N. Y. Ibrahim, and S. E. A. Elnahwy, "Second-order non-quasi-static, compact model of field-effect transistor revealing terminal rectification beyond their cutoff frequency," *IET Circuits Devices Syst.*, vol. 14, no. 5, pp. 660–666, Aug. 2020, doi: 10.1049/iet-cds.2019.0127.
[68] X. Liu, T. Ytterdal, and M. Shur, "Multi-Segment TFT Compact Model for THz Applications," *Nanomaterials*, vol. 12, no. 5, p. 765, Feb. 2022, doi: 10.3390/nano12050765.
[69] N. Y. Ibrahim, N. H. Rafat, and S. E. A. Elnahwy, "Multi-input intrinsic and extrinsic field effect transistor models beyond cutoff frequency," *Solid-State Electron.*, vol. 103, pp. 236–241, Jan. 2015, doi: 10.1016/j.sse.2014.07.006.
[70] F. Ludwig, M. Bauer, and A. Lisauskas, "Circuit-Based Hydrodynamic Modeling of AlGaN/GaN HEMTs," *ESSDERC 2019 - 49th Eur. Solid-State Device Res. Conf. ESSDERC*, p. 4.
[71] P. Földesy, "Current steering detection scheme of three terminal antenna-coupled terahertz field effect transistor detectors," *Opt. Lett.*, vol. 38, no. 15, p. 2804, Aug. 2013, doi: 10.1364/OL.38.002804.
[72] T. A. Elkhatib, V. Yu. Kachorovskii, W. J. Stillman, S. Rumyantsev, X.-C. Zhang, and M. S. Shur, "Terahertz response of field-effect transistors in saturation regime," *Appl. Phys. Lett.*, vol. 98, no. 24, p. 243505, Jun. 2011, doi: 10.1063/1.3584137.
[73] D. But, "Silicon based terahertz radiation detectors," *Charles Coulomb Lab. – UMR 5221 CNRS-Univ. Montp. 2*, p. 104.
[74] P. Földesy, "Terahertz responsivity of field-effect transistors under arbitrary biasing conditions," *J. Appl. Phys.*, vol. 114, no. 11, p. 114501, Sep. 2013, doi: 10.1063/1.4821250.